AIAA JOURNAL
Vol. 34, No. 6, June 1996

Stability of Leading-Edge Vortex Pair on a Slender Delta Wing

Ming-Ke Huang* and Chuen-Yen Chow†
University of Colorado, Boulder, Colorado 80309

A stability analysis is presented for a vortex pair over a highly swept flat-plate delta wing, by use of a formulation based on the slender-body theory for an inviscid incompressible flow. The vortex pair is found to be truly stable to all disturbances of small amplitude. The stabilizing mechanism has been identified to be the freestream velocity component that tends to pull the vortex pair toward the midplane of the delta wing. Such a mechanism is three dimensional in nature and cannot be provided by a two-dimensional stabilizing device. This result, together with a deduction that the strength of the vortex pair that can be trapped above a delta wing decreases with increasing sweepback angle, generally agrees with laboratory observations.

I. Introduction

THE idea of trapping a free vortex above a wing for lift augmentation has prompted both theoretical and experimental investigations. For example, Saffman and Sheffield[1] showed analytically that a vortex could be trapped by a flat-plate airfoil to greatly increase the lift. Rossow[2] suggested a method by using a vertical flap near the leading edge to generate a spanwise vortex on the upper surface of a wing, which was maintained stationary by the application of suction through orifices in endplates at the wingtip. Such a device could produce theoretical lift coefficients as high as 10, and some of the predicted vortical flow phenomena were identified in the laboratory. An extensive review of the literature on various geometrical and aerodynamical techniques for vortex trapping is contained in Rossow's recent papers.[3,4]

To have any practical applications, a free vortex must be stably trapped above the wing, in the sense that the vortex should return to its equilibrium position when displaced by an arbitrary disturbance. Under the assumption of two-dimensional small perturbations, the stability of a trapped vortex was examined by Saffman and Sheffield[1] for a flat-plate airfoil and by Huang and Chow[5] for a more general case of Joukowski airfoils. Locations at which the vortex became stable were computed, depending on the airfoil configuration, flight attitude, and vortex strength. Unfortunately, these were all neutrally stable locations and were valid only for displacements of infinitesimal amplitude. When a vortex trapped by a Joukowski airfoil was perturbed from its predicted stable position with a finite displacement, according to the numerical computation by Chow et al.,[6] the vortex tended to move initially around its original equilibrium position but eventually would be carried far downstream by the external flow. A similar behavior was also observed in Rossow's numerical result[2] for the case even when the equilibrium position was behind a leading-edge flap. Thus the neutrally stable locations predicted by the linear theory were shown to be actually unstable to realistic disturbances whose amplitudes were not necessarily small.

It appears that in a two-dimensional configuration a spanwise free vortex cannot be trapped stably even by use of external devices such as the surface suction examined by Chow et al.[7] or the dual-fence arrangement with a spanwise suction suggested by Rossow[3,4] and verified in the laboratory by Riddle et al.[8] On the other hand, stably trapped vortices have been observed in three-dimensional configurations. One of the well-known examples is the line-vortex pair formed by flow separation at the leading edge of a slender delta wing at high angles of attack.[9] These vortices, which will provide an additional vortex lift, are truly stable on a highly swept wing in that they will quickly return to the original equilibrium position after being perturbed. In the apparent absence of published work on the stability of the vortex pair, an analytical investigation of this problem is presented here in an attempt to identify the stabilizing mechanism for the delta wing.

Our stability study is based on a small-perturbation analysis of an inviscid and incompressible flow past a highly swept delta wing. In the presence of a pair of line vortices on the wing, the flowfield and the condition under which the vortices become trapped are first derived in Sec. II within the framework of slender-body theory. The vortices in the pair are then perturbed from their equilibrium location with an arbitrary disturbance of small amplitude, which is decomposed into four basic modes to facilitate the subsequent analysis. In Sec. III the complex growth rate for each of the four modes is obtained in closed form by solving the corresponding eigenvalue problem. Stability behaviors of these modes are examined in Sec. IV through numerical computation, and the final conclusions are given in Sec. V.

II. Potential Flow over Slender Delta Wing with a Vortex Pair

A. Slender-Body Approximation

Consider the flow past a flat-plate delta wing with half-apex angle ϵ at a high angle of attack. A body-fixed coordinate system is taken as shown in Fig. 1, where the y and z axes are along the wing span and centerline, respectively, and the x axis is normal to the planform surface. The freestream velocity V_∞ is inclined at angle of attack α with respect to the z axis. When the angle of attack is sufficiently large, flow separation occurs at the sharp leading edges to form a pair of swirling vortices. To simplify the analysis, the separation vortices are replaced by two straight vortex lines originated from the wing apex, with a circulation varying along the vortex axis. The velocity potential ϕ of the assumed inviscid incompressible flow is governed by the Laplace equation

$$\frac{\partial^2\phi}{\partial x^2}+\frac{\partial^2\phi}{\partial y^2}+\frac{\partial^2\phi}{\partial z^2}=0 \tag{1}$$

The angle ϵ is small for a slender wing, about which the flow varies slowly in the z direction. According to the slender-body theory,[10] the third term in Eq. (1) can be ignored in comparison with the other two terms. The governing equation is thus simplified to

$$\frac{\partial^2\phi}{\partial x^2}+\frac{\partial^2\phi}{\partial y^2}=0 \tag{2}$$

In other words, the velocity potential ϕ can be determined approximately in each crossflow plane by use of a complex potential.

It should be pointed out that the present simplified modeling of the separation vortices is essentially that used by Legendre[11] and Adams.[12] Such modeling was criticized[12,13] because there existed a pressure jump across the cut joining the leading edge and the vortex

Received Aug. 22, 1994; revision received June 12, 1995; accepted for publication July 27, 1995. Copyright © 1995 by the American Institute of Aeronautics and Astronautics, Inc. All rights reserved.

*Visiting Professor, Department of Aerospace Engineering Sciences; currently Professor, Department of Aerodynamics, Nanjing University of Aeronautics and Astronautics, Nanjing, 210016, People's Republic of China.

†Professor, Department of Aerospace Engineering Sciences. Associate Fellow AIAA.

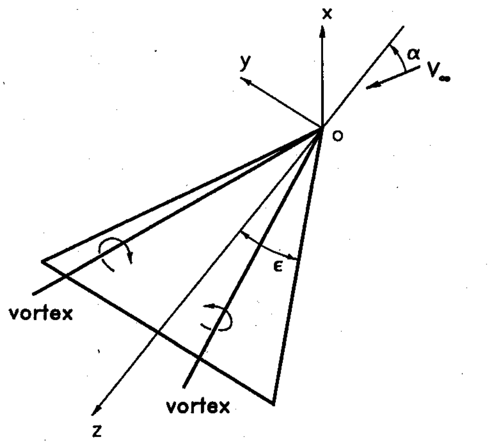

Fig. 1 Delta wing and coordinate system.

line due to a logarithmic singularity of the vortex. As a result, the lift obtained by pressure integration over the wing was different from that by the impulse method of Munk to include the lift on the cut. Nevertheless, instead of being used for the prediction of wing lift, this simplified model serves adequately the purpose of making a stability analysis.

B. Complex Potential in Crossflow Plane

We now consider an arbitrary crossflow plane perpendicular to the wing centerline, in which the local semispan of the wing is denoted by s. Figure 2a shows the physical $Z(= x + iy)$ plane that has been rotated so that the vertical x axis now becomes horizontal, along which the freestream crossflow velocity is $V_n = V_\infty \sin\alpha$. To obtain the complex potential W, the flow past a flat plate in the Z plane is mapped by the transformation

$$Z = \tfrac{1}{2}\left[\zeta - (s^2/\zeta)\right] \tag{3}$$

into that past a circle in the $\zeta(= \xi + i\eta)$ plane, as shown in Fig. 2b. Since $(\mathrm{d}Z/\mathrm{d}\zeta)_\infty = \frac{1}{2}$, the freestream crossflow velocity in the ζ plane is $V_n/2$. The complex potential of the flow in the ζ plane is

$$W(\zeta) = \frac{V_n}{2}\left(\zeta + \frac{s^2}{\zeta}\right) + \frac{i\Gamma}{2\pi}\left[\log\frac{\zeta-\zeta_0}{\zeta-\bar{\zeta}_0} - \log\frac{\zeta - (s^2/\bar{\zeta}_0)}{\zeta - (s^2/\zeta_0)}\right] \tag{4}$$

where Γ is the vortex circulation; and ζ_0 and $\bar{\zeta}_0$ are, respectively, the complex coordinates of the vortices outside the circle of radius s in the ζ plane. The magnitude of Γ is determined by the Kutta condition that flow velocity must vanish at $\zeta = is$, which transforms into a sharp edge in the Z plane. From this requirement, the dimensionless circulation is obtained as

$$\frac{\Gamma}{\pi s V_n} = \frac{\left(s^2 + |\zeta_0|^2\right)^2 - 4s^2\eta_0^2}{2\eta_0\left(|\zeta_0|^2 - s^2\right)s} \tag{5}$$

where $\zeta_0 = \xi_0 + i\eta_0$ transforms through Eq. (3) into the vortex position Z_0 in the physical plane.

C. Condition for the Separation Vortex to Become Stationary

The motion of the vortex pair is influenced by the crossflow $V_\infty \sin\alpha$ as well as by the chordwise flow $V_\infty \cos\alpha$. The complex velocity of the free vortex at Z_0 is

$$u_0 - iv_0 = \lim_{Z\to Z_0}\frac{\mathrm{d}}{\mathrm{d}Z}\left[W(\zeta) - \frac{i\Gamma}{2\pi}\log(Z - Z_0)\right] - \frac{V_n}{sK}\bar{Z}_0 \tag{6}$$

Here the first group on the right is the well-known expression due to the crossflow, and the last term represents the contribution from the axial velocity and is derived as follows.

In the plane containing two symmetrically situated vortex lines above a delta wing, Fig. 3 shows the left vortex line originated from the apex of the wing that makes an angle θ with the centerline.

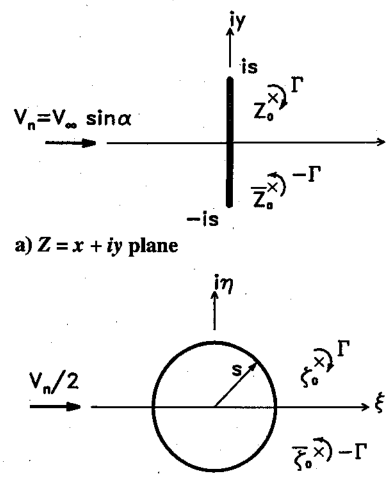

a) $Z = x + iy$ plane

b) $\zeta = \xi + i\eta$ plane

Fig. 2 Conformal mapping.

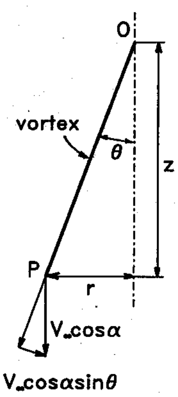

Fig. 3 Decomposition of the axial freestream velocity.

Consider a point P on the vortex line at a distance r from the centerline in the crossflow plane, whose distance from the apex is z. The chordwise velocity $V_\infty \cos\alpha$ at P has a component $V_\infty \cos\alpha \sin\theta$ perpendicular to the vortex line, whose component in the crossflow plane pointing toward the midplane of the delta wing has a magnitude

$$V_\infty \cos\alpha \sin\theta\cos\theta = V_\infty \cos\alpha\,(r/z)\cos^2\theta$$
$$= V_n(\tan\epsilon/\tan\alpha)(r/s)\cos^2\theta$$

In slender-body approximation, $\cos^2\theta \approx 1$, and with the introduction of the similarity parameter

$$K = \tan\alpha/\tan\epsilon \tag{7}$$

as suggested by Sychev,[14] that velocity component becomes

$$(V_n/K)(r/s)$$

which gives the last term on the right of Eq. (6) when expressed in terms of complex variables. It will be shown later that this velocity component, which tends to pull the vortex pair toward the midplane of the wing, plays an important role in stabilizing the vortex pair. Without it a stable trapping of the separation vortex lines is not possible.

After taking a limiting process,[2,10] Eq. (6) is reduced to

$$u_0 - iv_0 = (p_0 - iq_0)\left(\frac{\mathrm{d}\zeta}{\mathrm{d}Z}\right)_{Z=Z_0} - \frac{i\Gamma}{4\pi}\left[\frac{(\mathrm{d}^2Z/\mathrm{d}\zeta^2)}{(\mathrm{d}Z/\mathrm{d}\zeta)^2}\right]_{\zeta=\zeta_0} - \frac{V_n}{K}\frac{\bar{Z}_0}{s} \tag{8}$$

where

$$p_0 - iq_0 = \lim_{\zeta\to\zeta_0}\frac{\mathrm{d}}{\mathrm{d}\zeta}\left[W(\zeta) - \frac{i\Gamma}{2\pi}\log(\zeta - \zeta_0)\right] \tag{9}$$

represents the vortex velocity in the ζ plane, which, upon substitution of W from Eq. (4), is reduced to

$$p_0 - iq_0 = \frac{V_n}{2}\left(1 - \frac{s^2}{\zeta_0^2}\right) - \frac{i\Gamma}{2\pi}\left[\frac{1}{\zeta_0 - (s^2/\bar{\zeta}_0)} + \frac{1}{\zeta_0 - \bar{\zeta}_0} - \frac{1}{\zeta_0 - (s^2/\zeta_0)}\right] \tag{10}$$

For the vortex to become stationary, it is required that

$$u_0 - iv_0 = 0 \tag{11}$$

The two algebraic equations contained in Eq. (11) together with Eq. (5) form a nonlinear system that is used to solve for ξ_0, η_0, and Γ.

III. Stability Analysis of the Vortex Pair

Having determined the equilibrium position and strength of the vortex pair, we now proceed to examine the stability of the pair using a small-perturbation analysis. Each trapped vortex is treated as a free vortex whose circulation remains unchanged after it is displaced from its equilibrium position.

When the trapped vortex pair is perturbed slightly in the crossflow plane, vortices of much weaker strength will be shed from the sharp edges of the plate to satisfy the Kutta condition at those locations. Consider such a shed vortex in the ζ plane, which is initially situated on the imaginary axis at a short distance outside the circle of radius s shown in Fig. 2b. Its mirror image, which is a vortex of equal but opposite circulation, is also situated on the imaginary axis but at a short distance inside the circle. The influence of this weak shed vortex, in the presence of the canceling effect of its mirror image, is negligibly small in comparison with the mutual influences between the two trapped vortices in computing their subsequent motions. The following stability analysis is thus based on a formulation in which the shed vortices are ignored altogether. The same simplification has been adopted elsewhere, for example, in Refs. 1, 2, and 5, to facilitate the stability analyses of a single vortex trapped by various airfoil configurations.

A. Motion of the Perturbed Vortex Pair

In the crossflow plane, the vortex at Z_0 and that at $\bar{Z}_0$ are designated vortex 1 and vortex 2, respectively. The originally stationary vortices 1 and 2 are then given small displacements ΔZ_1 and ΔZ_2, corresponding, respectively, to $\Delta\zeta_1$ and $\Delta\zeta_2$ in the ζ plane. The complex velocity of vortex 1 in the Z plane is

$$u_1 - iv_1 = \lim_{\zeta\to\zeta_0+\Delta\zeta_1} \frac{\mathrm{d}}{\mathrm{d}Z}\left[W(\zeta) - \frac{i\Gamma}{2\pi}\log(Z - Z_0 - \Delta Z_1)\right] - \frac{V_n}{K}\frac{\overline{Z_0 + \Delta Z_1}}{s} \tag{12}$$

where

$$W(\zeta) = \frac{V_n}{2}\left(\zeta + \frac{s^2}{\zeta}\right) + \frac{i\Gamma}{2\pi}\left[\log(\zeta - \zeta_0 - \Delta\zeta_1) - \log\left(\zeta - \frac{s^2}{\overline{\zeta_0 + \Delta\zeta_1}}\right)\right] - \frac{i\Gamma}{2\pi}\left[\log(\zeta - \bar{\zeta}_0 - \Delta\zeta_2) - \log\left(\zeta - \frac{s^2}{\overline{\zeta_0 + \Delta\zeta_2}}\right)\right] \tag{13}$$

It can be reduced further to

$$u_1 - iv_1 = (p_1 - iq_1)\left(\frac{\mathrm{d}\zeta}{\mathrm{d}Z}\right)_{Z_0+\Delta Z_1} - \frac{i\Gamma}{4\pi}\left[\frac{(\mathrm{d}^2Z/\mathrm{d}\zeta^2)}{(\mathrm{d}Z/\mathrm{d}\zeta)^2}\right]_{\zeta_0+\Delta\zeta_1} - \frac{V_n}{K}\frac{\overline{Z_0 + \Delta Z_1}}{s} \tag{14}$$

where

$$p_1 - iq_1 = \lim_{\zeta\to\zeta_0+\Delta\zeta_1}\frac{\mathrm{d}}{\mathrm{d}\zeta}\left[W(\zeta) - \frac{i\Gamma}{2\pi}\log(\zeta - \zeta_0 - \Delta\zeta_1)\right]$$

$$= \frac{V_n}{2}\left[1 - \frac{s^2}{(\zeta_0 + \Delta\zeta_1)^2}\right] - \frac{i\Gamma}{2\pi}\left[\left(\zeta_0 + \Delta\zeta_1 - \frac{s^2}{\overline{\zeta_0 + \Delta\zeta_1}}\right)^{-1} - (\zeta_0 + \Delta\zeta_1 - \bar{\zeta}_0 - \Delta\zeta_2)^{-1} + \left(\zeta_0 + \Delta\zeta_1 - \frac{s^2}{\overline{\zeta_0 + \Delta\zeta_2}}\right)^{-1}\right] \tag{15}$$

Now we let

$$u_1 - iv_1 = Q(\Delta\zeta_1, \overline{\Delta\zeta_1}, \Delta\zeta_2, \overline{\Delta\zeta_2}) \tag{16}$$

and in view of the fact that the vortex pair is initially stationary, we have

$$Q(0, 0, 0, 0) = 0$$

A Taylor's series expansion gives

$$Q(\Delta\zeta_1, \overline{\Delta\zeta_1}, \Delta\zeta_2, \overline{\Delta\zeta_2}) = \left(\frac{\partial Q}{\partial\Delta\zeta_1}\right)_1\Delta\zeta_1 + \left(\frac{\partial Q}{\partial\overline{\Delta\zeta_1}}\right)_1\overline{\Delta\zeta_1} + \left(\frac{\partial Q}{\partial\Delta\zeta_2}\right)_1\Delta\zeta_2 + \left(\frac{\partial Q}{\partial\overline{\Delta\zeta_2}}\right)_1\overline{\Delta\zeta_2} \tag{17}$$

where only the first-order quantities are kept for small displacements, and $(\,)_1$ denotes the value evaluated at $\zeta = \zeta_0$, which is the equilibrium position of vortex 1. The motion of vortex 1 in the ζ plane is described by

$$\frac{\mathrm{d}\overline{\Delta\zeta_1}}{\mathrm{d}t} = \overline{\left(\frac{\mathrm{d}\zeta}{\mathrm{d}Z}\right)_1}\frac{\mathrm{d}\bar{Z}}{\mathrm{d}t} = Q(\Delta\zeta_1, \overline{\Delta\zeta_1}, \Delta\zeta_2, \overline{\Delta\zeta_2})\overline{\left(\frac{\mathrm{d}\zeta}{\mathrm{d}Z}\right)_1}$$

or

$$\frac{\mathrm{d}\overline{\Delta\zeta_1}}{\mathrm{d}t} = \left(\frac{\partial Q}{\partial\Delta\zeta_1}\right)_1\overline{\left(\frac{\mathrm{d}\zeta}{\mathrm{d}Z}\right)_1}\Delta\zeta_1 + \left(\frac{\partial Q}{\partial\overline{\Delta\zeta_1}}\right)_1\overline{\left(\frac{\mathrm{d}\zeta}{\mathrm{d}Z}\right)_1}\overline{\Delta\zeta_1} + \left(\frac{\partial Q}{\partial\Delta\zeta_2}\right)_1\overline{\left(\frac{\mathrm{d}\zeta}{\mathrm{d}Z}\right)_1}\Delta\zeta_2 + \left(\frac{\partial Q}{\partial\overline{\Delta\zeta_2}}\right)_1\overline{\left(\frac{\mathrm{d}\zeta}{\mathrm{d}Z}\right)_1}\overline{\Delta\zeta_2} \tag{18}$$

Equations (14) and (15) reveal that only $p_1 - iq_1$ depends on all of the four increments, namely, $\Delta\zeta_1$, $\overline{\Delta\zeta_1}$, $\Delta\zeta_2$, and $\overline{\Delta\zeta_2}$, whereas the remaining terms depend on $\Delta\zeta_1$ only. The required partial derivatives are given in the Appendix. Substitution of those derivatives into Eq. (18) gives

$$\frac{\mathrm{d}\overline{\Delta\zeta_1}}{\mathrm{d}\tau} = A\Delta\zeta_1 + \left(B - \frac{1}{K}\right)\overline{\Delta\zeta_1} + C\Delta\zeta_2 + D\overline{\Delta\zeta_2} \tag{19}$$

where

$$\tau = \frac{tV_n}{s} \tag{20}$$

is a dimensionless time, and

$$A = \frac{(s/V_n)\{[\partial(p_1 - iq_1)/\partial\Delta\zeta_1]\}_1(\mathrm{d}Z/\mathrm{d}\zeta)_1 - [s(p_1 - iq_1)/V_n](\mathrm{d}^2Z/\mathrm{d}\zeta^2)_1}{|\mathrm{d}Z/\mathrm{d}\zeta|_1^2(\mathrm{d}Z/\mathrm{d}\zeta)_1} - \frac{i\Gamma}{4\pi V_n s}\left[\frac{s^2(\mathrm{d}^3Z/\mathrm{d}\zeta^3)}{\mathrm{d}Z/\mathrm{d}\zeta|\mathrm{d}Z/\mathrm{d}\zeta|^2} - 2\frac{s^2(\mathrm{d}^2Z/\mathrm{d}\zeta^2)^2}{|\mathrm{d}Z/\mathrm{d}\zeta|^2(\mathrm{d}Z/\mathrm{d}\zeta)^2}\right]_1 \tag{21}$$

$$B = \frac{i\Gamma}{2\pi V_n s}\frac{s^4}{\left(|\zeta_0|^2 - s^2\right)^2}\left|\frac{\mathrm{d}Z}{\mathrm{d}\zeta}\right|_1^{-2} \tag{22}$$

$$C = -\frac{i\Gamma}{2\pi V_n s}\frac{s^2}{(\zeta_0 - \bar{\zeta}_0)^2}\left|\frac{\mathrm{d}Z}{\mathrm{d}\zeta}\right|_1^{-2} \tag{23}$$

$$D = -\frac{i\Gamma}{2\pi V_n s}\frac{s^4}{\left(\zeta_0^2 - s^2\right)^2}\left|\frac{\mathrm{d}Z}{\mathrm{d}\zeta}\right|_1^{-2} \tag{24}$$

Here $p_1 - iq_1$ and $\partial(p_1 - iq_1)/\partial\Delta\zeta_1$ are given in Eqs. (A3) and (A2) of the Appendix. The terms A, B, C, and D are dimensionless coefficients, of which A and D are complex and B and C are purely imaginary. These coefficients are to be evaluated for given geometric and fluid dynamic parameters.

The transformation derivatives shown in Eqs. (21–24) are obtained from Eq. (3),

$$\frac{\mathrm{d}Z}{\mathrm{d}\zeta} = \frac{1}{2}\left(1 + \frac{s^2}{\zeta^2}\right) \tag{25}$$

$$\frac{\mathrm{d}^2Z}{\mathrm{d}\zeta^2} = -\frac{s^2}{\zeta^3} \tag{26}$$

$$\frac{\mathrm{d}^3Z}{\mathrm{d}\zeta^3} = \frac{3s^2}{\zeta^4} \tag{27}$$

The equation of motion for vortex 2 is derived in a similar manner, which reads

$$\frac{\mathrm{d}\Delta\zeta_2}{\mathrm{d}\tau} = D\Delta\zeta_1 + C\overline{\Delta\zeta}_1 + \left(B - \frac{1}{K}\right)\Delta\zeta_2 + A\overline{\Delta\zeta}_2 \tag{28}$$

B. Decomposition of a General Disturbance

Displacements $\Delta\xi_1$ and $\Delta\xi_2$ of vortices 1 and 2 along the ξ axis can be in either the same or opposite directions, and the same holds also for displacements $\Delta\eta_1$ and $\Delta\eta_2$ along the η axis. Linear combinations of these arrangements result in four basic modes as sketched in Fig. 4, which can be synthesized to represent any arbitrary disturbance in the ξ–η plane. Of these four, only mode I is symmetric in the sense that the displacements are mirror images about the wing symmetric plane, and the other three are all asymmetric modes. The eigenvalues for the four modes are derived in the following, from which the inherent stability behavior of each mode can be deduced.

C. Eigenvalue Problem

Let us examine Eqs. (19) and (28), which are the equations describing the motions of a pair of vortices in the transformed circle plane when perturbed slightly from their trapped stationary position. By taking the real and imaginary parts of these two complex equations, four simultaneous equations are obtained that can be written in the following matrix form:

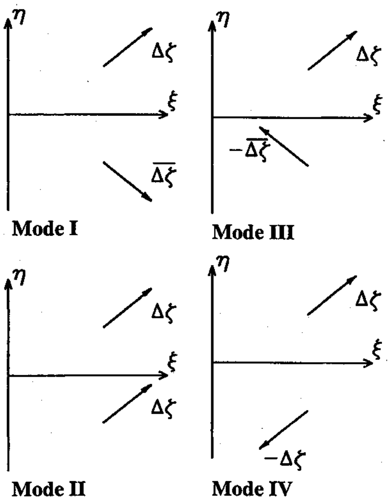

Fig. 4 Four basic disturbance modes.

The coefficients in this equation are all real, but their expressions are too long to be shown here. The four roots, λ_1, λ_2, λ_3, and λ_4, of Eq. (31) represent, respectively, the eigenvalues for the four modes listed in Fig. 4. When any one of the eigenvalues is found to have a positive real part, the corresponding mode represents an unstable disturbance. Thus for the stability of a general disturbance, it is required that the real parts of all four eigenvalues be negative.

IV. Computational Results

The stability of a pair of vortices trapped symmetrically above a slender delta wing is examined for values of K covering a wide range of the combination of angle of attack and aspect ratio. These two parameters are related through K defined in Eq. (7), by virtue of the fact that the aspect ratio of a delta wing is given by $4\tan\epsilon$.

For a given value of K, the stability computations are carried out as follows: The nonlinear system of Eqs. (5) and (11) are solved first to obtain the circulation $\Gamma/(sV_n)$ and the equilibrium position $(\xi_0/s, \eta_0/s)$ for one of the vortices in the ζ plane. The vortex location $(x_0/s, y_0/s)$ in the physical crossflow plane is determined through transformation (3). Coefficients A, B, C, and D are then evaluated from Eqs. (21–24), from which the eigenvalues for the four possible disturbance modes are finally determined by computing the roots of the quartic equation (31) based on the formulas given in Ref. 15.

Computations have been carried out for values of K ranging from 0.2 to 2.0. As K increases, the captured vortex pair will move upward from the wing surface and, in the meantime, shift inward from the wing tip region as shown in Fig. 5, but they can never be inside the spanwise station at 75.8% of the semispan on either side of the wing. The figure also indicates that stronger vortices are trapped at distances higher above the wing.

$$\frac{\mathrm{d}}{\mathrm{d}\tau}\begin{pmatrix}\Delta\xi_1\\ \Delta\eta_1\\ \Delta\xi_2\\ \Delta\eta_2\end{pmatrix} = \begin{pmatrix}\mathrm{Re}(A) - K^{-1} & -\mathrm{Im}(A - B) & \mathrm{Re}(D) & -\mathrm{Im}(C - D)\\ -\mathrm{Im}(A + B) & -\mathrm{Re}(A) - K^{-1} & -\mathrm{Im}(C + D) & \mathrm{Re}(D)\\ \mathrm{Re}(D) & \mathrm{Im}(C - D) & \mathrm{Re}(A) - K^{-1} & \mathrm{Im}(A - B)\\ \mathrm{Im}(C + D) & \mathrm{Re}(D) & \mathrm{Im}(A + B) & -\mathrm{Re}(A) - K^{-1}\end{pmatrix}\begin{pmatrix}\Delta\xi_1\\ \Delta\eta_1\\ \Delta\xi_2\\ \Delta\eta_2\end{pmatrix} \tag{29}$$

To determine the stability of the vortex pair, we specifically look for the solutions of the preceding homogeneous system of equations containing a common factor $\exp(\lambda\tau)$. Here λ is an eigenvalue of the coefficient matrix H on the right-hand side of Eq. (29) and is a root of the characteristic equation

$$\det(H - \lambda I) = 0 \tag{30}$$

where I is the identity matrix. Expansion of the characteristic determinant leads to the following quartic equation:

$$\lambda^4 + c_3\lambda^3 + c_2\lambda^2 + c_1\lambda + c_0 = 0 \tag{31}$$

When the vortex pair is perturbed from the equilibrium position with disturbances shown in Fig. 4, the eigenvalues of the four modes governing the subsequent motions are calculated and plotted in Fig. 6. As revealed in that figure, λ_1 and λ_2 are complex conjugates, λ_3 and λ_4 are real double roots, and, interestingly, the real parts of all four eigenvalues assume the same negative value for any given value of K. Thus it is concluded that the vortex pair is stable to any small-amplitude disturbance formed by a linear combination of the four basic modes described in Fig. 4.

We have indicated in the Introduction that a free vortex trapped in any two-dimensional configuration is at most neutrally stable,

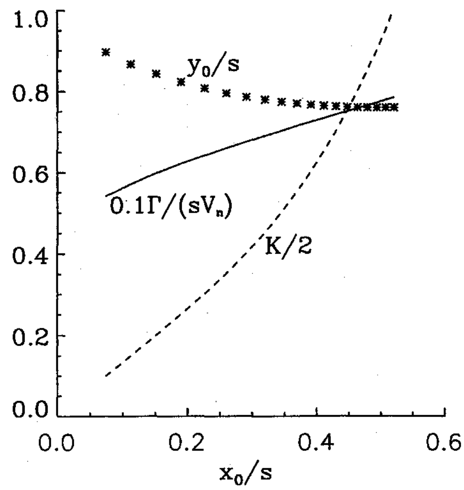

Fig. 5 Effect of varying K on properties of vortex trapped above delta wing.

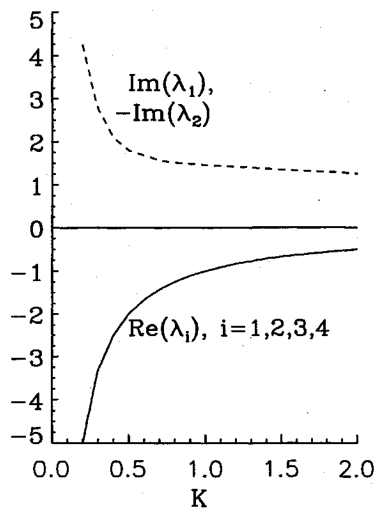

Fig. 6 Eigenvalues for modes I–IV.

owing to the fact that the eigenvalues for stability are purely imaginary with a vanished real part. Let us now find the mechanism that causes a true stability of the vortex pair in a three-dimensional configuration, under which any initial disturbance is damped in time. A close examination of the computational procedure reveals that the stabilizing effect is attributed to the negative real term $-K^{-1}$ that shows in every root λ of the quartic equation (31), which is a direct consequence of the fact that this term appears in all diagonal elements of the coefficient matrix H in Eq. (30). Physically, this term is originated from the chordwise velocity component $V_\infty \cos\alpha$ of the freestream (see Fig. 3), which tends to pull the vortex pair toward the midplane of the delta wing. Such a stabilizing mechanism is three dimensional in nature and thus cannot be provided by a two-dimensional stabilizing device. It has already been shown that a truly stable condition cannot be achieved for a free vortex trapped in two-dimensional configuration by using vortex fences[2–4] or by applying surface suction.[7]

Figure 6 shows that the stability of the trapped vortex pair is enhanced by reducing $K(=\tan\alpha/\tan\epsilon)$, which can be attained either by decreasing the angle of attack of a given swept wing or by increasing the apex angle of a delta wing for a fixed angle of attack. However, when α is decreased to be below a certain value, the flow can no longer separate from the leading edge, so that the assumed vortex pair does not even exist, or when the apex angle increases continuously, the slender-wing approximation may finally be violated. In either case, K approaches zero and the present analysis becomes invalid.

In addition to the stability analysis, we now examine the dependence of leading-edge vortex strength on leading-edge sweep as deduced from the present computation, in comparison with the results obtained from experiment and other theories. Hemsch and

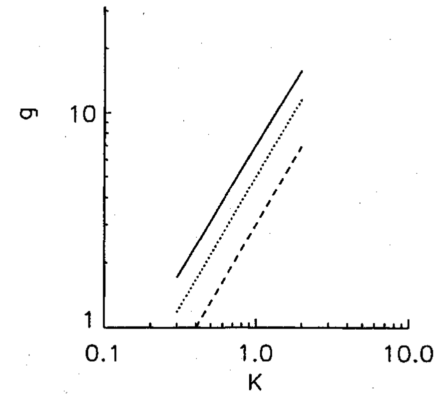

Fig. 7 Variation of g with K for delta wings. Solid line represents the present theory; dotted and dashed lines represent, respectively, the theoretical and experimental data correlated by Hemsch and Luckring.[16]

Luckring[16] correlated some low-speed experimental data that were fitted with the dashed line shown in the logarithmical plot of g vs K in Fig. 7, in which $g = \Gamma K/sV_n$ is a dimensionless circulation. The solid line in Fig. 7 represents the result of the present work, and the dotted line describes a power law of the form

$$g \sim K^{1.2} \tag{32}$$

which was deduced from the numerical results of Smith[17] based on a conical slender-body theory.

A quantitative comparison of these three curves does not seem appropriate because of the different assumptions involved in the theoretical analyses and the way in which the experimental circulation data were acquired in the laboratory. Nevertheless, the fact that all three curves are parallel indicates that they follow the same power law described in Eq. (32) but with different constants of proportionality. From the definitions of g and K, for a delta wing of length l at a fixed angle of attack, Eq. (32) can be rewritten as

$$(\Gamma/V_\infty l) \sim (\tan\epsilon)^{0.8} \tag{33}$$

It shows that the strength of the trapped vortices decreases with increasing leading-edge sweep, which is in agreement with the observation described in Ref. 16.

V. Conclusions

The vortices separated from the sharp leading edge of a highly swept flat-plate delta wing at high angle of attack are modeled as two straight vortex lines originated from the wing apex. Based on a potential flow analysis under slender-body approximations, the strength and equilibrium location of the line vortices are determined. Stability of the trapped vortex pair is studied by examining its response to small disturbances in a crossflow plane perpendicular to the wing centerline. With an arbitrary disturbance decomposed into four basic modes, it is found that the vortex pair is always stable. The analysis reveals that the stabilizing effect is caused by the component of the freestream velocity that tends to pull the vortex pair toward the central symmetric plane of the wing. The analysis also indicates that the circulation of the trapped vortices decreases with increasing sweep angle of the wing. All of the theoretically predicted phenomena are supported by laboratory observations.

Appendix: Some Derivatives Needed for Stability Analysis

$$\left(\frac{\partial Q}{\partial \Delta\zeta_1}\right)_1 = \frac{\{[\partial(p_1 - iq_1)/\partial\Delta\zeta_1]\}_1 (\mathrm{d}Z/\mathrm{d}\zeta)_1 - (p_1 - iq_1)(\mathrm{d}^2Z/\mathrm{d}\zeta^2)_1}{(\mathrm{d}Z/\mathrm{d}\zeta)_1^2}$$
$$- \frac{i\Gamma}{4\pi}\left[\frac{(\mathrm{d}^3Z/\mathrm{d}\zeta^3)}{(\mathrm{d}Z/\mathrm{d}\zeta)^2} - 2(\mathrm{d}Z/\mathrm{d}\zeta)\frac{(\mathrm{d}^2Z/\mathrm{d}\zeta^2)^2}{(\mathrm{d}Z/\mathrm{d}\zeta)^4}\right]_{\zeta=\zeta_0} - \frac{V_n}{Ks}\frac{\overline{\Delta Z_1}}{\Delta\zeta_1} \tag{A1}$$

where

$$\left(\frac{\partial(p_1 - iq_1)}{\Delta\zeta_1}\right)_1 = \frac{V_n s^2}{\zeta_0^3} + \frac{i\Gamma}{2\pi} \times \left[\frac{1}{(\zeta_0 - \bar{\zeta}_0)^2} + \frac{1}{\left[\zeta_0 - \left(s^2/\bar{\zeta}_0\right)\right]^2} - \frac{1}{\left[\zeta_0 - \left(s^2/\zeta_0\right)\right]^2}\right] \tag{A2}$$

and

$$(p_1 - iq_1)_1 = \frac{V_n}{2}\left(1 - \frac{s^2}{\zeta_0^2}\right) - \frac{i\Gamma}{2\pi}\left[\frac{1}{\zeta_0 - \left(s^2/\bar{\zeta}_0\right)} + \frac{1}{\zeta_0 - \bar{\zeta}_0} - \frac{1}{\zeta_0 - \left(s^2/\zeta_0\right)}\right] \tag{A3}$$

$$\left(\frac{\partial Q}{\partial \overline{\Delta\zeta}_1}\right)_1 = \left[\frac{\partial(p_1 - iq_1)}{\partial \overline{\Delta\zeta}_1}\right]_1 \left(\frac{\mathrm{d}\zeta}{\mathrm{d}Z}\right)_1 = \frac{i\Gamma}{2\pi}\frac{s^2}{\left(|\zeta_0|^2 - s^2\right)^2}\left(\frac{\mathrm{d}\zeta}{\mathrm{d}Z}\right)_1 \tag{A4}$$

$$\left(\frac{\partial Q}{\partial \Delta\zeta_2}\right)_1 = \left[\frac{\partial(p_1 - iq_1)}{\partial \Delta\zeta_2}\right]_1 \left(\frac{\mathrm{d}\zeta}{\mathrm{d}Z}\right)_1 = -\frac{i\Gamma}{2\pi}\frac{1}{\left(\zeta_0 - \bar{\zeta}_0\right)^2}\left(\frac{\mathrm{d}\zeta}{\mathrm{d}Z}\right)_1 \tag{A5}$$

$$\left(\frac{\partial Q}{\partial \overline{\Delta\zeta}_2}\right)_1 = \left[\frac{\partial(p_1 - iq_1)}{\partial \overline{\Delta\zeta}_2}\right]_1 \left(\frac{\mathrm{d}\zeta}{\mathrm{d}Z}\right)_1 = -\frac{i\Gamma}{2\pi}\frac{s^2}{\left(\zeta_0^2 - s^2\right)^2}\left(\frac{\mathrm{d}\zeta}{\mathrm{d}Z}\right)_1 \tag{A6}$$

References

[1]Saffman, P. G., and Sheffield, J. S., "Flow over a Wing with an Attached Free Vortex," *Studies in Applied Mathematics*, Vol. 57, No. 2, 1977, pp. 107–117.

[2]Rossow, V. J., "Lift Enhancement by an Externally Trapped Vortex," *Journal of Aircraft*, Vol. 15, No. 9, 1978, pp. 618–625.

[3]Rossow, V. J., "Two-Fence Concept of Efficient Trapping of Vortices on Airfoils," *Journal of Aircraft*, Vol. 29, No. 5, 1992, pp. 847–855.

[4]Rossow, V. J., "Aerodynamics of Airfoils with Vortex Trapped by Two Spanwise Fences," *Journal of Aircraft*, Vol. 31, No. 1, 1994, pp. 146–153.

[5]Huang, M. K., and Chow, C. Y., "Trapping of a Free Vortex by Joukowski Airfoils," *AIAA Journal*, Vol. 20, No. 3, 1982, pp. 292–298.

[6]Chow, C. Y., Huang, M. K., and Yan, C. Z., "Unsteady Flows About a Joukowski Airfoil in the Presence of Moving Vortices," *AIAA Journal*, Vol. 21, No. 5, 1985, pp. 657, 658.

[7]Chow, C. Y., Chen, C. L., and Huang, M. K., "Trapping of a Free Vortex by Airfoils with Surface Suction," *AIAA Journal*, Vol. 24, No. 8, 1986, pp. 1217, 1218.

[8]Riddle, T. W., Wadcock, A. J., Tso, J., and Cummings, R. M., "Experimental Analysis of Trapping Techniques," AIAA Paper 91-3271, Sept. 1991.

[9]Lowson, M. V., "Some Experiments with Vortex Breakdown," *Journal of the Aeronautical Society*, Vol. 68, May 1964, pp. 343–346.

[10]Nielson, J. N., *Missile Aerodynamics*, McGraw–Hill, New York, 1960.

[11]Legendre, R., "Écoulement au Voisinage De La Pointe Avant D'une Aile A Forte Fléche Aux Incidences Moyennes," *La Recherche Aeronautique*, Bulletin Bimestriel, De L'Office National D'Études Et De Recherches Aéronautiques, Nov.–Dec. 1952 and Jan.–Feb. 1953.

[12]Adams, M. C., "Leading-Edge Separation from Delta Wing at Supersonic Speeds," *Journal of the Aeronautical Sciences*, Vol. 20, No. 6, 1953, pp. 430, 431.

[13]Brown, C. E., and Michael, W. H., Jr., "On Slender Wings with Leading Edge Separation," NACA TN 3430, April 1955.

[14]Sychev, V. V., "Three-Dimensional Hypersonic Gas Flow Past Slender Bodies at High Angles of Attack," *Journal of Mathematics and Mechanics* (USSR), Vol. 24, Feb. 1960, pp. 296–306.

[15]Pearson, C. E., *Handbook of Applied Mathematics*, Van Nostrand Reinold, New York, 1974, pp. 13, 14.

[16]Hemsch, M. J., and Luckring, J. M., "Connection Between Leading-Edge Sweep, Vortex Lift and Vortex Strength for Delta Wings," *Journal of Aircraft*, Vol. 27 , No. 5, 1990, pp. 473–475.

[17]Smith, J. H. B., "Calculations of the Flow over Thick, Conical, Slender Wings with Leading-Edge Separation," Aeronautical Research Council, ARC R&M 3694, London, March 1972.